Journal of Molecular Spectroscopy 261 (2010) 68–71

Contents lists available at ScienceDirect

Journal of Molecular Spectroscopy

journal homepage: www.elsevier.com/locate/jms

Note

The [1 + 1] two-photon dissociation spectra of $CO_2^+(X^2\Pi_g(\Omega = 3/2))$ via $A^2\Pi_{u,3/2}(\upsilon_1\upsilon_2 0) \leftarrow X^2\Pi_{g,3/2}(000)$ transitions

Maoping Yang, Limin Zhang *, Danna Zhou, Qian Sun

Department of Chemical Physics, University of Science and Technology of China, Hefei, Anhui 230026, People's Republic of China

ARTICLE INFO

Article history:
Received 19 January 2010
In revised form 9 March 2010
Available online 17 March 2010

Keywords:
CO_2^+
Two-photon dissociation spectra
Vibronic bands

ABSTRACT

The mass-resolved [1 + 1] two-photon dissociation spectra of $CO_2^+(X^2\Pi_g(\Omega = 3/2))$ via $A^2\Pi_{u,3/2}(\upsilon_1\upsilon_2 0) \leftarrow X^2\Pi_{g,3/2}(000)$ transitions were studied by introducing a dissociation laser with a wavelength of 283–353 nm. $CO_2^+(X^2\Pi_{g,3/2}(000))$ was prepared by the [3 + 1] multiphoton ionization of CO_2 at 333.69 nm. The vibronic bands of $(\upsilon_1 20; \upsilon_1 = 0\text{–}5)\mu^2\Pi_{3/2}$ and $(\upsilon_1 20; \upsilon_1 = 0\text{–}5)\kappa^2\Pi_{3/2}$ involving the bending mode of $CO_2^+(A^2\Pi_{u,3/2})$ were assigned. Based on the assignments, the spectral constants of $T_e = 27969.3 \pm 1.2\ cm^{-1}$ [above $CO_2^+(X^2\Pi_{g,3/2})$], $\nu_1 = 1125.89 \pm 0.53\ cm^{-1}$, $\chi_{11} = -0.659 \pm 0.010\ cm^{-1}$, $\nu_2(\mu^2\Pi_{3/2}) = 429.5 \pm 9.7\ cm^{-1}$, and $\nu_2(\kappa^2\Pi_{3/2}) = 528.7 \pm 8.0\ cm^{-1}$ for $CO_2^+(A^2\Pi_{u,3/2})$ were deduced. The photodissociation dynamics of CO_2^+ via $A^2\Pi_{u,3/2}(\upsilon_1\upsilon_2 0) \leftarrow X^2\Pi_{g,3/2}(000)$ transitions are discussed.

The linear triatomic CO_2^+ ion is an important component in planetary atmospheres [1], and its spectroscopy and dynamic behavior have attracted the attention of experimenters and theoreticians [2]. The vibronic structures of $CO_2^+\left(X^2\Pi_g, A^2\Pi_u, B^2\Sigma_u^+, C^2\Sigma_g^+\right)$ have been investigated previously using various experimental techniques, including emission [3–5], laser absorption [6,7], HeI photoelectron [8–15], threshold photoelectron (TPE) [16,17], photoionization efficiency [18–20], photoelectron–photon coincidence [21], photoion–photon coincidence [22], photoelectron–photoion coincidence [23], pulsed field ionization (PFI)–photoelectron (PFI-PE) [24–28], PFI-PE-photoion (PFI-PE-PI) coincidence [29] measurements, and resonance enhanced multiphoton ionization [30,31]. However, there are few reports on the vibronic level-selected excitation and dissociation spectroscopy for CO_2^+, which could provide more detailed information for the photochemistry of CO_2^+ in a direct way compared to the photoelectron spectra of neutral molecule. In our previous study, we obtained the [1 + 1] two-photon dissociation spectra of $CO_2^+(X^2\Pi_g(\Omega = 1/2))$ via $A^2\Pi_{u,1/2}(\upsilon_1\upsilon_2 0) \leftarrow X^2\Pi_{g,1/2}(000)$ transitions [32]. Because the (000) band intensity of $CO_2^+(X^2\Pi_g(\Omega = 3/2))$ is much weaker than that of $CO_2^+(X^2\Pi_g(\Omega = 1/2))$, a higher signal to noise ratio is needed to study $CO_2^+(X^2\Pi_g(\Omega = 3/2))$ ions. In this study, we present a similar study on the [1 + 1] two-photon dissociation spectra of $CO_2^+(X^2\Pi_g(\Omega = 3/2))$ with a pulsed tunable laser with a wavelength range of 283–353 nm. By combining data from this study with the data from our previous study, more integrated data on the $A^2\Pi_u$ state of CO_2^+ was obtained.

The experimental setup has been previously described [32–34]. Jet-cooled CO_2 molecules were produced by supersonic expansion of pure CO_2 gas at about 3 atm through a pulsed nozzle (General Valve) with a nozzle orifice diameter of 0.5 mm and were introduced into a photoionization chamber. The ionization laser at 333.69 nm was perpendicularly focused on the molecular beam of CO_2 by a quartz lens with $f = 135$ mm to produce a CO_2^+ ion via [3 + 1] resonance-enhanced multiphoton ionization (REMPI) of CO_2 molecules [30,31]. The dissociation laser (~0.2 mJ/pulse) at 283–353 nm counterpropagating with the ionization laser was focused by a quartz lens with $f = 320$ mm to excite $CO_2^+(X^2\Pi_{g,3/2})$. Both lasers were temporally and spatially matched with each other at the laser-molecular interaction point. The wavelength of the lasers was calibrated using a wavemeter.

The ions were extracted and accelerated into a TOF (time of flight) mass spectrometer and drifted along a 70 cm long TOF tube. The ions were detected by a microchannel plate (MCP) detector, and the signals from the MCP output were amplified by a preamplifier (Stanford model SR240A). The mass-resolved data were collected by averaging the amplified signals for the selected mass species with a transient recorder and stored in a personal computer. The intensities of the ionization laser and the dissociation lasers were monitored simultaneously during the experiment.

As revealed by Wu and co-workers [35], in the resonance-enhanced multiphoton ionization photoelectron spectrum (REMPI-PES) of CO_2 via $3p\pi_u\,^1\Delta_u(\Omega = 3/2)$ spin–orbit state, the (000) level of $CO_2^+(X^2\Pi_{g,3/2})$ is much stronger than those related to the higher vibrational levels of $CO_2^+(X^2\Pi_{g,3/2})$ (see Fig. 1b in Ref. [35]). In this study, the CO_2^+ ions were prepared in $X^2\Pi_{g,3/2}(000)$ states with minimum amounts of CO^+, O^+, and C^+ ions, with a lens with $f = 135$ mm to focus the ionization laser (~5 mJ/pulse) at 333.69 nm. The involved [3 + 1] REMPI process of CO_2 to prepare $CO_2^+(X^2\Pi_{g,3/2}(000))$ ions has been previously described [30,31].

* Corresponding author.
E-mail address: lmzha@ustc.edu.cn (L. Zhang).

0022-2852/$ - see front matter © 2010 Elsevier Inc. All rights reserved.
doi:10.1016/j.jms.2010.03.006

$$CO_2\left(X^1\Sigma_g^+\right) \xrightarrow{3h\nu} CO_2(3p\pi_u\,{}^1\Delta_u(3/2)) \xrightarrow{h\nu} CO_2^+\left(X^1\Pi_{g,3/2}(000)\right) + e.$$

The mass-resolved photodissociation spectra (the depletion spectrum of parent ion CO_2^+ and the enhanced spectrum of fragment ions CO^+, O^+, and C^+) in Fig. 1 were obtained by scanning the dissociation laser in the range of 283–353 nm. Based on the spectroscopy of CO_2^+ previously reported [3,4,15,27,28,36], the photodissociation spectra could be completely assigned as the electronic transition of $CO_2^+(A^2\Pi_{u,3/2}(\upsilon_1\upsilon_2 0)) \leftarrow CO_2^+(X^2\Pi_{g,3/2}(000))$, where υ_1 and υ_2 represent vibrational quantum numbers for the ν_1 (symmetric stretching) and ν_2 (bending) modes, respectively. The possible assignments of the photodissociation spectra shown in Fig. 1 are summarized in Table 1. Note that the photodissociation spectra can be complicated by vibration–electronic interaction (Renner–Teller effect) and Fermi resonance interaction related to $CO_2^+(A^2\Pi_{u,3/2}(\upsilon_1\upsilon_2 0))$. The vibration–electronic interaction induces the Renner–Teller splitting of a $^2\Pi$ state (lower μ and upper κ components of $A^2\Pi_{u,3/2}$ in Table 1) whenever the bending vibration ν_2 is excited [37]. Because the vibrational frequencies of $CO_2^+(A^2\Pi_{u,3/2})$ have the approximate relationship $\nu_1 \sim 2\nu_2$, a group of vibrational levels involving the symmetric stretch ν_1 and overtones of the bending vibration ν_2, such as the (υ_1,0,0) and (υ_1-1,2,0) levels of CO_2^+ ($A^2\Pi_{u,3/2}$) can be coupled through strong Fermi resonances. Because of the strong Fermi resonance interaction, the unfavorable Franck–Condon transitions $A^2\Pi_{u,3/2}(\upsilon_1\text{-}1,2,0) \leftarrow X^2\Pi_{g,\,3/2}(000)$ can occur with comparable intensities due to strongly allowed transitions $A^2\Pi_{u,\,3/2}(\upsilon_1 00) \leftarrow X^2\Pi_{g,\,3/2}(000)$, which is indicated in Fig. 1.

As shown in Table 1, the ν_{expt} values of $A(\upsilon_1 00;\ \upsilon_1 = 0-6)^2\Pi_{3/2}$, A(020; 520) $\mu^2\Pi_{3/2}$, and A(020; 320; 420; 520) $\kappa^2\Pi_{3/2}$ are in good agreement with the known ν_{PES} values [28]. Based on the data for the $A^2\Pi_{u,1/2} \leftarrow X^2\Pi_{g,1/2}$ transition in our previous study and the $A^2\Pi_{u,3/2} \leftarrow X^2\Pi_{g,3/2}$ transition presented in this work, it is now possible to identify several unresolved $A(\upsilon_1\upsilon_2 0)$ $\mu^2\Pi_{3/2,1/2}$ and $A(\upsilon_1\upsilon_2 0)$ $\kappa^2\Pi_{3/2,1/2}$ bands [28]. For example, we could certainly give the resolved ν_{expt} values of A(120, 220, 320, 420) $\mu^2\Pi_{3/2}$ and A(120, 220) $\kappa^2\Pi_{3/2}$ bands to improve the unresolved ν_{PES} values of the A(120, 220, 320, 420) $\mu^2\Pi_{3/2,1/2}$ and A(120, 220) $\kappa^2\Pi_{3/2,1/2}$ bands in Ref. [28].

The spectral constants of $T_e = 27969.3 \pm 1.2\ cm^{-1}$ [above $CO_2^+(X^2\Pi_{g,3/2})$], $\nu_1 = 1125.89 \pm 0.53\ cm^{-1}$, $\chi_{11} = -0.659 \pm 0.010\ cm^{-1}$, $\nu_2(\mu^2\Pi_{3/2}) = 429.5 \pm 9.7\ cm^{-1}$, and $\nu_2(\kappa^2\Pi_{3/2}) = 528.7 \pm 8.0\ cm^{-1}$ for $CO_2^+(A^2\Pi_{u,3/2})$ were deduced from the $A^2\Pi_{u,\,3/2}(\upsilon_1\upsilon_2 0) \leftarrow X^2\Pi_{g,3/2}(000)$ transitions of CO_2^+. The deduced vibrational frequencies for $CO_2^+(A^2\Pi_{u,3/2})$ are in accordance with those of $\nu_1 = 1127\ cm^{-1}$, and $\nu_2 = 461\ cm^{-1}$ given by emission spectra [3,4] and PFI-PE [28] spectra.

In addition, the spectral band of $B^2\Sigma_u^+(000) \leftarrow X^2\Pi_{g,3/2}(000)$ was also observed due to the overlap between $A^2\Pi_{u,3/2}$ and $B^2\Sigma_u^+$.

Considering that the one-photon excitation energy (3.51–4.38 eV) related to the resonance peaks in Fig. 1 cannot access the dissociation limit of CO_2^+ for the formation of O^+ (5.2738 eV), CO^+ (5.6724 eV) [29], and C^+ (6.98 eV) [38] from its electronic ground state, two photon excitation energy (7.02–8.76 eV) is needed to dissociate CO_2^+. This means that the dissociation process of CO_2^+ via $A^2\Pi_{u,3/2}(\upsilon_1\upsilon_2\ 0) \leftarrow X^2\Pi_{g,3/2}(000)$ transitions to produce CO^+, O^+, and C^+ is a [1 + 1] two-photon process, that is, the intermediate state in this photodissociation process is the $A^2\Pi_{u,3/2}$ state of CO_2^+.

Fig. 1 shows that CO^+ is the main ionic product in the [1 + 1] photodissociation process of CO_2^+ compared to O^+ and C^+. Moreover, the C^+ yield is higher than the O^+ yield, even though the dissociation limit to form O^+ is the lowest. The percentage branching ratios of $[CO^+]/([CO^+] + [O^+] + [C^+])$, $[C^+]/([CO^+] + [O^+] + [C^+])$, and $[O^+]/([CO^+] + [O^+] + [C^+])$ measured in this work in the two photon energy range of 57000–70600 cm^{-1} are shown in Fig. 2. The $[CO^+]/([CO^+] + [O^+] + [C^+])$ percentage branching ratio of 69–79% is much larger than the percentage branching ratios of $[C^+]/([CO^+] + [O^+] + [C^+])$ and $[O^+]/([CO^+] + [O^+] + [C^+])$, which were 14–20% and 6–11%, respectively. Similar photofragment branching ratios were also observed for the $(\upsilon_1 + 1,\ 0,\ 0)^2\Pi_{3/2}$, $(\upsilon_1,\ 2,0)\mu^2\Pi_{3/2}$, and $(\upsilon_1,\ 2,0)\kappa^2\Pi_{3/2}$ bands.

Since CO^+ is the main ionic product compared to O^+ for the ionization energy of CO_2 exceeding 19.5000 eV [5.7235 eV above $CO_2^+(X^2\Pi_{g,3/2}(000))$] [29] in the PFI-PEPICO experiment, it is reasonable to assume that the dissociation dynamics for the vibrationally excited levels of $CO_2^+(C^2\Sigma_g^+)$ [39,29] are also applicable in the internal energy range of 7.02–8.76 eV above $CO_2^+(X^2\Pi_{g,3/2}(000))$. In terms of energy, a two photon energy of 7.02–8.76 eV can reach the high vibrational levels in the $(C^2\Sigma_g^+)^\dagger$ state via the allowed transitions of $(C^2\Sigma_g^+)^\dagger \leftarrow A^2\Pi_{u,1/2} \leftarrow X^2\Pi_{g,1/2}$, where the superscript "†" denotes high vibrational levels in the corresponding electronic states. In addition, both the repulsive CO_2^+ ($b^4\Pi_u/{}^4B_1$) state connected with $CO^+(X^2\Sigma^+) + O(^3P_g)$ and the repulsive CO_2^+ ($a^4\Sigma_g^-$) state connected with $O^+(^4S_u) + CO(X^1\Sigma^+)$ cover the energy range of 7.02–8.76 eV, where $b^4\Pi_u/{}^4B_1$ represents either $^4\Pi_u$ for the linear geometry or $^4B_1$ for the bent geometry (more stable geometry for this state) [39]. Thus, the dissociation should depend on the ways to reach $CO_2^+(b^4\Pi_u/{}^4B_1)$ or $CO_2^+(a^4\Sigma_g^-)$. The direct transitions of $b^4\Pi_u/{}^4B_1 \leftarrow A^2\Pi_u$ and $a^4\Sigma_g^- \leftarrow A^2\Pi_u$ are forbidden by selection rules of $u \leftarrow | \rightarrow u$ or/and $S = 3/2 \leftarrow | \rightarrow S = 1/2$. Additionally, the direct predissociation of $CO_2^+(C^2\Sigma_g^+)$ ions via the $a^4\Sigma_g^-$ state to form $O^+(^4S) + CO(X^1\Sigma^+)$ is not possible because the spin–orbit coupling integral for these states $\langle a^4\Sigma_g^+, m_s = 3/2 \mid \mathbf{L}\cdot\mathbf{S} \mid C^2\Sigma_g^+, m_s = 1/2\rangle$ gives no contribution for $\Delta m_s = 1$. Moreover, the predissociation of the vibrationally excited $CO_2^+(C^2\Sigma_g^+)^\dagger$ state at energies above the second dissociation limit CO^+ $(X^2\Sigma^+) + O(^3P_g)$ can take place via the repulsive $b^4\Pi_u/{}^4B_1$ state because the spin–orbit coupling between these two electronic states is highly efficient ($\approx$40 cm^{-1}). Other ways leading to $O^+(^4S_u) + CO(X^1\Sigma^+)$ by coupling between $CO_2^+(b^4\Pi_u/{}^4B_1)$ and $CO_2^+(a^4\Sigma_g^-)$, which leads to $CO^+(X^2\Sigma^+) + O(^3P_g)$ by the spin–orbit interaction between $CO_2^+(b^4\Pi_u/{}^4B_1)$ and $CO_2^+(X^2\Pi_g)^\dagger$ are also possible.

As indicated by the branching ratios of 7.2–11.5 for $[CO^+]/[O^+]$, a strong preference in the [1 + 1] photodissociation process to form CO_2^+ is observed for the formation of the $CO^+(X^2\Sigma^+) + O(^3P_g)$ channel compared to the formation of the lowest product channel $O^+(^4S_u) + CO(X^1\Sigma^+)$. This fact can be rationalized by the more efficient spin–orbit couplings between this state and the $b^4\Pi_u/{}^4B_1$ state because $CO_2^+(C^2\Sigma_g^+)^\dagger$ is prepared in states at 7.02–8.76 eV.

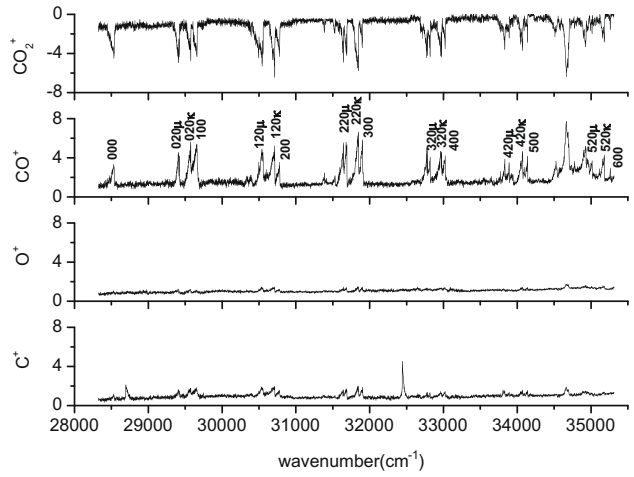

Fig. 1. The mass-resolved [1 + 1] photodissociation spectra of CO_2^+ obtained in the wavelength range of 283–353 nm. The spectra are assigned to the $A^2\Pi_{u,3/2}(\upsilon_1\upsilon_2 0) \leftarrow X^2\Pi_{g,3/2}(000)$ transitions of CO_2^+.